

Quantum Channel Polynomial Processing

Tianhan Liu,* Fedor Šimkovic IV, and Martin Leib

IQM Quantum Computers, Georg-Brauchle-Ring 23-25, 80992 Munich, Germany

(Dated: July 8, 2026)

We introduce a quantum algorithmic framework based on probabilistic mixtures of unitary channels that, similar to the framework of quantum singular value transformations, enables the application of arbitrary polynomials of hermitian operators onto arbitrary initial states. We show that our framework supports a flexible tradeoff between sample- and query complexity ranging from optimal query complexity, meaning logarithmic in the error, and exponentially scaling sample complexity to sub-polynomial query complexity in the error and polynomial sample complexity. Combined with the considerably lower quantum circuit complexity, compared to quantum singular value transformations with a linear combination of unitaries block encoding, we argue that our framework can be seamlessly scaled from NISQ to fault-tolerant quantum computing.

I. INTRODUCTION

Quantum algorithms are expected to provide asymptotic advantages over classical counterparts for a range of problems, including quantum search [1, 2], factoring [3], quantum simulation [4, 5], and differential equations [6]. A recurring primitive in many of these algorithms is the implementation of functions of an operator, and in particular functions of a Hamiltonian, $f(H)$, within a quantum process [7]. Polynomial approximation provides a natural route to this task: a target function f is approximated by a polynomial of degree d , after which the problem becomes one of realizing the corresponding polynomial transformation of the Hamiltonian H on quantum hardware.

Quantum singular value transformation (QSVT) provides a powerful coherent realization of this idea. Given access to a suitable unitary encoding of H , QSVT implements polynomial transformations of the encoded operator using $\mathcal{O}(d)$ applications of the underlying unitary, where d is the degree of the approximating polynomial. When such an encoding is available, this scaling makes QSVT an asymptotically optimal framework in the query model. Together with the theory of polynomial approximation and interpolation [8, 9], QSVT and related block-encoding techniques provide a central theoretical framework for Hamiltonian simulation [5], ground-state preparation [10], thermal-state preparation [11], matrix arithmetic [12], and other Hamiltonian-function algorithms.

The practical use of QSVT is limited by the need to encode the Hamiltonian of interest into a unitary operation. In conventional block-encoding approaches, such as linear combination of unitaries (LCU) [5, 13, 14] or sparse-matrix encodings [15], the coefficients of Hamiltonian terms or sparse matrix entries are loaded into ancillary registers, often using quantum read-only memory (QROAM) [16], while controlled operations select the corresponding unitary terms. For quantum chemistry Hamiltonians, where the number of terms typically

scales as $\mathcal{O}(N^4)$, such coherent selection procedures imply substantial ancillary overhead, many controlled operations, and large Toffoli counts. As a result, the standard block-encoded route to QSVT is most naturally suited to large-scale fault-tolerant quantum computers.

Several approaches seek to reduce this overhead while remaining within the block-encoding framework. Rather than coherently selecting from a generic list of Hamiltonian terms, these methods exploit additional structure of the operator to simplify state preparation, control logic, or the encoded representation itself. Examples include variational block-encoding methods [17], tensor-network encodings of matrix product operators [18], Dicke-state-based constructions [19], and chemistry-specific encodings [20–23]. While these approaches can lower particular resource costs, they still require a coherent unitary encoding of the Hamiltonian, and their efficiency depends on optimization, compressibility, or problem-specific algebraic structure.

A distinct approach is to avoid coherent Hamiltonian encoding and represent the Hamiltonian statistically through sampled circuits. Product formulas, or Trotterization [24, 25], implement Hamiltonian dynamics by applying gates generated by individual Hamiltonian terms, with circuit complexity depending on the target precision [26] and the number of Hamiltonian terms. Randomized product formulas such as QDrift [27–29] replace deterministic traversal over Hamiltonian terms by probabilistic sampling, thereby trading part of the circuit depth for repetitions; in suitable regimes, the sampling cost can be controlled using concentration properties of martingale processes [30]. Randomized LCU methods [31–33] apply a related sampling principle to conditional Pauli circuits. These methods show that coherent Hamiltonian selection can be replaced by stochastic circuit ensembles in certain settings. However, they are primarily designed for Hamiltonian time evolution or sampled LCU constructions, and do not directly provide a general polynomial-transformation framework for arbitrary functions, $f(H)$, and they often entail an exponential sampling overhead.

This leaves an algorithmic gap between block-encoded polynomial transformations and stochastic Hamiltonian

* tianhan.liu@iqm.tech

simulation. QSVT provides a general polynomial framework but relies on coherent unitary block encodings of the Hamiltonian. Product-formula and randomized simulation methods reduce coherent circuit requirements by using sampled circuits, but their structure is not naturally adapted to arbitrary Hamiltonian functions. The question is therefore whether polynomial Hamiltonian-function approximation can be combined with stochastic circuit sampling, without constructing a deterministic coherent block encoding of H .

In this work, we introduce a stochastic quantum algorithm framework called quantum channel polynomial processing (QCPP) for implementing Hamiltonian functions in quantum channels. The construction follows the polynomial-approximation perspective underlying QSP, while replacing coherent block encoding by stochastic encodings of Hamiltonian commutators and anti-commutators at the channel level. These encodings are then used to formulate a corresponding signal-processing procedure for target functions of Hamiltonians. For a degree- d interpolating polynomial, each sampled circuit contains at most $2d$ conditional Pauli rotations, while additional Hamiltonian terms enter through the sampling distribution rather than through coherent selection hardware.

This formulation shifts the resource requirements from coherent Hamiltonian selection to stochastic sampling. Each circuit instance is substantially simpler than a conventional block-encoded QSP circuit and avoids many of the coherent-control requirements that dominate standard implementations [34], while sampling complexity becomes the relevant additional resource. Thus, our proposed QCPP method occupies a different point in the algorithmic design space: it retains the use of polynomial approximations to target Hamiltonian functions while trading coherent circuit complexity for repetitions. We study the sample complexity of this stochastic compilation procedure for real- and imaginary-time evolution as a low-resource application. The resulting circuit structures indicate a route toward implementing QSVT-inspired Hamiltonian-function methods on near- and intermediate-term quantum computers.

The paper is structured as follows: We start in Section II by introducing the general stochastic quantum algorithm framework of QCPP, explaining along the way how it implements polynomials of hermitian operators. In Section III we prove fundamental relationships illustrating the sample- and query complexity tradeoffs of the method. We finish the article with general remarks in Section IV relating to commutativity and the relation of QCPP to QSVT and provide concluding thoughts in Section V.

II. ALGORITHM FRAMEWORK

To introduce our QCPP quantum algorithmic framework, we will start from two opposing directions: first

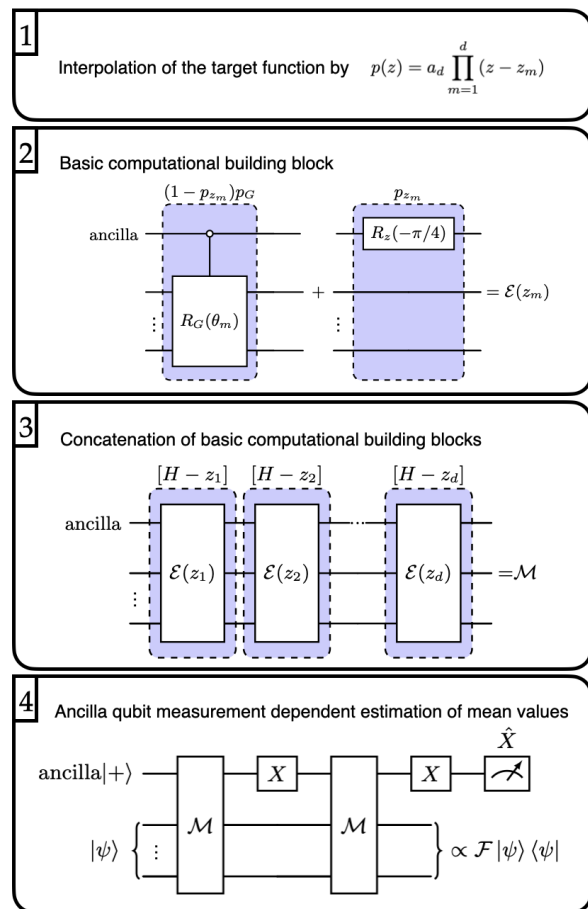


FIG. 1. Workflow of the Quantum Channel Polynomial Processing (QCPP) method: (1) A target function f is interpolated by a order- d polynomial p . (2) The basic computational building block of QCPP then corresponds to stochastically sampling unitary circuits, c.f. (3) Every basic computational building block corresponds to a root of the interpolating polynomial. To encode the entire polynomial one needs to concatenate d basic computational building blocks probabilities to construct the channel \mathcal{M} (4) Channel \mathcal{M} needs to be repeated twice with interleaved application of a X gate on the ancilla qubit. (5) Measurements on the computational register informed by the measurement result on the ancilla qubit enable the estimation of observables of the desired final state on the computational qubit register.

from a top down direction formulating the ultimate computational goal and second from the bottom up direction explaining the basic stochastic building block with the goal of illustrating how it needs to be employed to reach the algorithmic goal. The entire workflow is illustrated in Fig. 1.

A. Algorithmic Goal

A huge class of quantum algorithms can be described by applying a function f of a hermitian operator H on a

generic initial state ρ of an n -qubit computational register,

$$f(H)\rho f(H)^\dagger = f(\mathcal{A}_H - i\mathcal{C}_H)f^*(\mathcal{A}_H + i\mathcal{C}_H)\rho, \quad (1)$$

followed by a measurement on the resulting state. In anticipation of the introduction of the stochastic building block in the next subsection we reformulate the high level quantum algorithm in the superoperator picture with the help of the commutator $\mathcal{C}_H\rho = \frac{i}{2}[H, \rho]$ and anti-commutator $\mathcal{A}_H\rho = \frac{1}{2}\{H, \rho\}$ superoperators. These commute $\mathcal{C}_H\mathcal{A}_H\rho = \mathcal{A}_H\mathcal{C}_H\rho$ as long as we consider them with respect to the same operator H . We consider the hermitian operator H without loss of generality to be expressed as some real prefactor λ and a convex combina-

tion of a subset $S \subset G_n$ of signed n -qubit Pauli operators $G_n = \{\pm P_1 \otimes \dots \otimes P_n | P_i \in \{\mathbb{1}, Z, X, Y\}\}$ where Z, X and Y are the Pauli matrices, $H = \lambda \sum_{g \in S} p_g g$. All p_g are real and positive and sum up to 1, $\sum_{g \in S} p_g = 1$.

In the following, we will show how to implement a probabilistic quantum algorithm for functions f that are polynomials of finite degree d , $f \propto p(z) = a_d \prod_{i=1}^d (z - z_i)$, represented here in their factorized form with leading coefficient a_d and roots $\{z_i \in \mathbb{C} | p(z_i) = 0\}$, which is the step 1 in the workflow in Fig. ?? Therefore, for a general function f we need to find an interpolating polynomial p that approximates f on an appropriately defined interval such that,

$$f(H)\rho f(H)^\dagger \approx |a_d|^2 \prod_{i=1}^d (\mathcal{A}_H - i\mathcal{C}_H - z_i)(\mathcal{A}_H + i\mathcal{C}_H - z_i^*)\rho = |a_d|^2 \prod_{i=1}^d [(\mathcal{A}_H - \Re[z_i])^2 + (\mathcal{C}_H + \Im[z_i])^2] \rho = \mathcal{F}\rho. \quad (2)$$

In order to not make the nomenclature too cumbersome for the remainder of the article we will consider “normalized” Hamiltonians $H \rightarrow h/\lambda$ and assume interpolating polynomials approximating the appropriately rescaled function, $p(\cdot) \approx f(\lambda \cdot)$. With this convention it is sufficient that the interpolating polynomial is approximating the function f well on the interval $[-1, 1]$.

B. Probabilistic Building Block

To accomplish this task we consider the use of a computational building block inspired by the qDRIFT protocol [27] that consists of a probabilistic mixture of unitary channels,

$$\mathcal{E} = p_z[U_z] + (1 - p_z) \sum_{g \in S} p_g[cR_g(\theta)]. \quad (3)$$

Here, we are using the convention of square brackets to symbolize the mapping of a unitary operator to its corresponding unitary channel $[U](\rho) := U\rho U^\dagger$. To imple-

ment the desired parametrized unitaries we supplement a computational register hosting n qubits with an ancillary qubit. With probability p_z we execute a $\pi/4$ rotation along the z -axis on the ancilla qubit $\exp(i\frac{\pi}{4}z_a)$ and with probability $(1 - p_z)p_g$ we execute a rotation with generator g with an angle θ controlled by the ancilla qubit $cR_g(\theta) = \exp(i\theta(|1\rangle\langle 1|_a \otimes g) = \exp(i\theta(\frac{1}{2}(z_a + 1) \otimes g))$. Here we have introduced the convention of writing many body Pauli operators in the following way, $\sigma_i = \mathbb{1}_a \otimes \mathbb{1}_1 \otimes \dots \otimes \Sigma_i \otimes \dots \otimes \mathbb{1}$ for $(\sigma, \Sigma) \in \{(z, Z), (x, X), (y, Y)\}$. The circuit diagram of this computational building block is shown in Fig. 1 step 2.

To better understand the effect of the above defined computational building block on the computational register, we define a partial transfer matrix picture with respect to the ancilla qubit for an arbitrary channel \mathcal{E} , $[\mathcal{E}]_{\Sigma, \Delta}^{(\text{TM})} \rho = \text{tr}_a[\Sigma \otimes \mathbb{1} \mathcal{E}(\Delta \otimes \rho)]$ for $\{\Sigma, \Delta\} \in \{\mathbb{1}, Z, X, Y\}^{\otimes 2}$, where $\text{tr}_a[\cdot]$ is the partial trace with respect to the ancilla qubit. With this convention the above introduced algorithmic building block can be written as a direct sum $[\mathcal{E}]^{(\text{TM})} = \mathbf{A}_{\mathbb{1}-Z} \oplus \mathbf{B}_{X-Y}$ where,

$$\mathbf{A}_{\mathbb{1}-Z} = \begin{pmatrix} \frac{1-p_z}{2} \sum_{g \in S} p_g [R_g(\theta)] + \frac{1+p_z}{2} & \frac{1-p_z}{2} (\sum_{g \in S} p_g [R_g(\theta)] - 1) \\ \frac{1-p_z}{2} (\sum_{g \in S} p_g [R_g(\theta)] - 1) & \frac{1-p_z}{2} \sum_{g \in S} p_g [R_g(\theta)] + \frac{1+p_z}{2} \end{pmatrix}, \quad (4)$$

acts on the $\mathbb{1}$ - Z subspace and

$$\mathbf{B}_{X-Y} = (p_z - 1) \sin(\theta) \begin{pmatrix} \mathcal{C}_H - \cot(\theta) & \mathcal{A}_H - \frac{p_z}{(p_z-1)\sin(\theta)} \\ -(\mathcal{A}_H - \frac{p_z}{(p_z-1)\sin(\theta)}) & \mathcal{C}_H - \cot(\theta) \end{pmatrix}, \quad (5)$$

acts on the X - Y subspace, where $R_g(\theta) = \exp(i\theta g)$ is the

uncontrolled version of the unitary of the computational

building block.

C. Assembling the Building Blocks

Next, we show how to assemble the above introduced computational building block such that we are able to implement the desired channel of Eq. (2). As a first step we consider for the moment a polynomial of degree one ($d = 1$), and recognize that the determinant of \mathbf{B}_{X-Y} is proportional to the desired channel when we choose the angle $\theta \leftarrow \theta_1$ and probability $p_z \leftarrow p_{z_1}$ to be,

$$\theta_1 = \arctan\left(\frac{-1}{\Re[z_1]}\right), \quad (6)$$

and

$$p_{z_1} = \frac{\Re[z_1]}{\Re[z_1] + \sqrt{1 + \Im[z_1]^2}}, \quad (7)$$

which ultimately means that the basic computational building block is now a function of a specific root of the interpolating polynomial $\mathcal{E} \rightarrow \mathcal{E}(z_i)$. As a second step we realize that because of the direct sum structure of the basic computational building block in the partial Pauli transfer matrix picture the same structure also emerges when we start concatenating multiple computational building blocks,

$$[\mathcal{E}(z_p) \circ \dots \circ \mathcal{E}(z_1)]^{(\text{TM})} = \mathbf{A}(z_p) \dots \mathbf{A}(z_1) \oplus \mathbf{B}(z_p) \dots \mathbf{B}(z_1). \quad (8)$$

Combining the above two insights we can conclude that if we could somehow compute the determinant of the X - Y subspace of a channel that has the above described direct

sum structure we would be able to implement a channel on the computational register proportional to Eq. (2) because the determinant of the product of matrices is the product of their determinants, $\det(\mathbf{M}_1 \mathbf{M}_2 \dots \mathbf{M}_p) = \det(\mathbf{M}_1) \det(\mathbf{M}_2) \dots \det(\mathbf{M}_p)$. This product of the matrices is illustrated in step 3 in Fig. 1.

To see how we can compute the desired determinants we first define the following product: $D_K = Z \prod_{i \in K} \mathbf{B}_{X-Y}(\theta_i) Z \prod_{i \in K} \mathbf{B}_{X-Y}(\theta_i)$, such that K is a subset of the computational building blocks needed to implement the polynomial of Eq. (2). Note that for any subset K we have:

$$D_K \propto \prod_{i \in K} ((\mathcal{A}_H - \Re[z_i])^2 + (\mathcal{C}_H + \Im[z_i])^2) \mathbb{1} \quad (9)$$

such that the product of all D_{K_i} of any partition $\{K_i\}$ of the original set of d roots of the polynomial would lead to a proper computation of the determinant in the X - Y subspace. To implement a Pauli Z term in the X - Y subspace of the partial Pauli transfer matrix picture it suffices to apply an X gate to the ancilla qubit since, $[x_a]^{(\text{TM})} = Z_{1-Z} \oplus Z_{X-Y}$.

As a last step we need to make sure that we can apply the channel in the X - Y subspace on the computational register. To this end, we initialize the ancilla qubit in the $|+\rangle$ state and measure in the X basis. Initializing the ancilla qubit in the $|+\rangle$ state is in the partial Pauli transfer matrix picture equivalent to applying all matrices on the initial state, $[|+\rangle\langle+|]^{(\text{TM})} = [\frac{1}{2}(\mathbb{1} + X)]^{(\text{TM})} = (\frac{1}{2}, 0, \frac{1}{2}, 0)^T$ while measuring in the X -basis of the ancilla qubit is equivalent to collapsing the state into either $[|+\rangle\langle+|]^{(\text{TM})} = (\frac{1}{2}, 0, \frac{1}{2}, 0)$ or $[|-\rangle\langle-|]^{(\text{TM})} = (\frac{1}{2}, 0, -\frac{1}{2}, 0)$. There are no gates in the entire discussed circuit that change the amplitudes of the $|+\rangle$ and $|-\rangle$ states of the ancilla qubit such that the measurement probabilities for the respective outcomes are both $\frac{1}{2}$. This means we are ultimately implementing, on the computational register, a probabilistic mixture with equal probabilities of two channels:

$$\rho \rightarrow \frac{1}{2} \left(\underbrace{(1 \ 0) Z \mathbf{A}(\theta_d) \dots \mathbf{A}(\theta_1) Z \mathbf{A}(\theta_d) \dots \mathbf{A}(\theta_1)}_{\mathcal{P}} \begin{pmatrix} 1 \\ 0 \end{pmatrix} \pm \underbrace{(1 \ 0) Z \mathbf{B}(\theta_d) \dots \mathbf{B}(\theta_1) Z \mathbf{B}(\theta_d) \dots \mathbf{B}(\theta_1)}_{\mathcal{F}} \begin{pmatrix} 1 \\ 0 \end{pmatrix} \right) \rho. \quad (10)$$

For ease of illustration we have presented above a version of the expression with only two X -gates on the ancilla qubit. This step of the QCPP workflow is illustrated in step 4 in Fig. 1. However, the above formula can be generalized to any other partition $\{K_i\}$. This means that if we were to ignore the measurement results of the ancilla qubit, the desired channel \mathcal{F} would average out.

In an unraveling of the actual quantum measurement of an observable O we would measure eigenstates of O which do not correspond to the probabilities we would want to have, namely $p_i \propto \langle i | \mathcal{F} \rho | i \rangle$, but rather those of $q_i = \frac{1}{2} (\langle i | \mathcal{P} | i \rangle \pm p_i)$, depending on this measurement outcome of the ancilla. It is precisely the measurement outcome of the ancilla qubit that lets us tag the posi-

tive and negative outcomes which we can subsequently use to change the sign of the eigenvalue corresponding to the measured eigenstate of the observable to ultimately average out the unwanted channel \mathcal{P} .

III. SAMPLE- AND QUERY COMPLEXITY TRADEOFF

To estimate the mean value of an observable with respect to the above introduced stochastic framework we first need to calculate the actual factor of proportionality between the channel we want to implement and the channel we can implement,

$$\Gamma(p) := |a_d| \prod_{i=1}^d (\Re[z_i] + \sqrt{1 + \Im[z_i]}). \quad (11)$$

Using a standard argument for unbiased sampling we see that we need to measure at least M times such that $\sqrt{M} \gg \Gamma(p)$ to keep the additive error of the mean value approximation small. Therefore, we will call $\Gamma(p)$ from now on the sample complexity of QCPP. In addition to the sample complexity we should capture the query complexity or the number of ‘‘oracle calls’’ which is the number of basic computational building blocks d we choose to apply. The query complexity can also be seen to directly relate to the depth of the quantum circuit we need to execute. In the following, we argue that the optimal query complexity can be achieved for QCPP, but only at the cost of an exponentially growing sample complexity. We go on to construct a class of approximating polynomials that enable a variable tradeoff between sample and query complexity. Ultimately, we can show that upon increasing the query complexity polynomially we are able to get a super-algebraically decreasing additive error as well as an only polynomially growing sample complexity. Specifically, we generate these two insights for both real and imaginary time evolution.

A. Optimal Query Complexity for Real and imaginary Time Evolution

It is possible to get the optimal query complexity for real-, $f^{\text{real}}(z) = \exp(-itz) \approx p^{\text{real}}(z)$, and imaginary, $f^{\text{imag}}(z) = \exp(-\tau(z+1)) \approx p^{\text{imag}}(z)$, time evolution in terms of the respective simulated time, t or τ , as well as in terms of the additive precision of the approximation. This can be accomplished by using, for example, the respective Jacobi-Anger expansions,

$$p^{\text{imag}}(z) = e^{-\tau} (I_0(\tau) + 2 \sum_{n=1}^d (-1)^n I_n(\tau) T_n(z)) \quad (12)$$

$$p^{\text{real}}(z) = J_0(t) + 2 \sum_{n=1}^N (-i)^n J_n(t) T_n(z), \quad (13)$$

where J_n are the ordinary Bessel functions of first kind and I_n are the modified Bessel functions of first kind and T_n are the Chebyshev polynomials of first kind. However, as mentioned above it is possible to show that for both cases the sample complexity grows exponentially in d .

Theorem 1 Exponential sample cost of Jacobi-Anger expansions

Let $p^{\text{real}}(x)$ ($p^{\text{imag}}(x)$) be the Jacobi-Anger expansion of real (imaginary) time evolution truncated at degree d . Then it is possible to find constants c^{real} and c^{imag} , independent of d such that the sample complexity is growing at least exponentially in d ,

$$\Gamma(p^{\text{real}}) \in \Omega(\exp(c^{\text{real}}d)) \quad (14)$$

$$\Gamma(p^{\text{imag}}) \in \Omega(\exp(c^{\text{imag}}d)), \quad (15)$$

for real- and imaginary time evolution respectively.

For details of the proof we refer to the supplementary material. We were further also able to prove an exponentially growing upper bound and therefore show that the sample complexity for both real- and imaginary time evolution is exponentially growing as a function of the chosen query complexity d . For the proof of this theorem we also refer to the supplementary material. An important insight of the proof of Theorem 1 is that the sample complexity is growing exponentially in the number of roots of the interpolating polynomial that are neither lying on the positive real axis nor on the imaginary axis of the Gaussian plane. The proof then proceeds to show that for the majority of the roots of the truncated Jacobi-Anger expansion this is the case. We use this insight to construct interpolating polynomials in the next section that provide us with a flexible tradeoff between sample- and query complexity.

B. Flexible Tradeoff between Sample- and Query Complexity

We construct interpolating polynomials as products of two polynomials $p(x) = q(x)h(x)$. For this product we see that the sum of the degrees of the polynomials $\deg(q) = d_q$ and $\deg(h) = d_h$ is d and the sample complexity is the product of the sample complexities of the two polynomials, $\Gamma(p) = \Gamma(q)\Gamma(h)$. For q we choose a class of polynomials whose sample complexity is equal to 1. For the case of real- and imaginary time evolution these are, respectively,

$$q^{\text{real}}(z) = \frac{(1 - i \frac{t}{d_q} z)^{d_q}}{\left(1 + \frac{t^2}{d_q^2}\right)^{d_q/2}} \quad (16)$$

$$q^{\text{imag}}(z) = \frac{(1 - \frac{\tau}{d_q} z)^{d_q}}{\left(1 + \frac{\tau}{d_q}\right)^{d_q}}. \quad (17)$$

The sample complexity can be bounded because the roots of these polynomials are either on the imaginary or positive real axis of the Gaussian plane. In the case of real time evolution they are all the same and located on the imaginary axis $\{z_i\}_{i=1}^n = -in/t$. For imaginary time they are all identical as well and located on the positive real axis $\{z_i\}_{i=1}^n = n/\tau$. The remaining polynomial h we define to be the approximation of $h^{imag} \approx f^{imag}/q^{imag}$ and $h^{real} \approx f^{real}/q^{real}$ based on Chebyshev polynomials truncated at logarithmic d , $d_h \propto \log(d)$, respectively. With this construction it is obvious that the sample complexity is polynomial in the query complexity, that means the degree of the interpolating polynomial d . We were further able to show super-algebraic convergence for these specific polynomials on the relevant interval of $[-1, 1]$.

Theorem 2

Super-algebraic convergence

Let $q^{real/imag}$, $h^{real/image}$, and $f^{real/image}$ be defined as above, then the interpolating polynomial converges super-algebraically to the target function on the interval $[-1, 1]$

$$\|f^{real} - q^{real}h^{real}\|_{\infty} \leq C\left(\frac{t^2}{d}\right)d^{-\log d}, \quad (18)$$

$$\|f^{imag} - q^{imag}h^{imag}\|_{\infty} \leq C\left(\frac{\tau^2}{d}\right)d^{-\log d}, \quad (19)$$

where $\|f(x)\|_{\infty} = \sup_{x \in [-1, 1]} |f(x)|$ is the supremum norm on the interval $[-1, 1]$. $C(\frac{t^2}{d})$ and $C(\frac{\tau^2}{d})$ are constant functions in terms of the two ratios. For the proof of the theorem we refer to the supplementary material. Finally, given an upper bound of the sampling cost Γ_{\star} , we can also derive from this theorem the optimal query complexity:

$$d \sim \frac{t^2}{\log \Gamma_{\star}} + \log \frac{1}{\epsilon}, \quad d \sim \frac{\tau^2}{\log \Gamma_{\star}} + \log \frac{1}{\epsilon}, \quad (20)$$

for real and imaginary time evolution, which is supported by our numerical data as detailed in the supplementary material.

IV. GENERAL REMARKS

A. Commutative Structure

Note that basic computational building blocks do not commute for general angle values $\mathcal{E}(\theta_1)\mathcal{E}(\theta_2) \neq \mathcal{E}(\theta_2)\mathcal{E}(\theta_1)$. However, a permutation of the computational building blocks order does not have any effect on the relevant part of the quantum channel acting on the computational register. That means we are still implementing the desired channel \mathcal{F} on the computational register. This can be seen from at least two possible angles. First, it can be seen from the fact that the desired channel \mathcal{F} is a result of taking the determinant of a set of

computational building blocks and the fact that the determinant is actually permutation invariant for matrix products, $\det(\mathbf{M}_1\mathbf{M}_2) = \det(\mathbf{M}_2\mathbf{M}_1)$. Second, we can also see that every application of the basic computational building block is associated to a root of the polynomial we want to apply and the roots have no inherent order. This fact can be used to find more favorable transpilation techniques for various quantum hardware platforms. However, it might even hint at more fundamental insights about the general QCPP algorithm, similar to findings about instantaneous quantum polynomial circuits. In contrast to the desired channel \mathcal{F} , the other channel \mathcal{P} actually is not independent of the chosen sequence of the basic computational building blocks. The exact channel can be conveniently calculated by first considering the action of the entire quantum algorithm on an initial state that is a tensor product of the projectors onto computational basis states of the ancilla qubit, $|0\rangle\langle 0| \otimes \rho$. For every partition we realize that, thanks to the controlled rotation of $\mathcal{E}(\theta_i)$, only one of the two copies of the basis computational building blocks is actually acting on the computational register. Ultimately, we can determine the channel \mathcal{P} to be,

$$\mathcal{P} = \mathcal{E}'(\theta_d) \circ \dots \circ \mathcal{E}'(\theta_1), \quad (21)$$

where we have introduced,

$$\mathcal{E}'(\theta) = p_z + (1 - p_z) \sum_{G \in S} p_g [R_g(\theta)], \quad (22)$$

as the uncontrolled version of the basic computational building block.

B. Comparison with Quantum Singular Value Transformations

The here presented quantum algorithmic framework bears close resemblance with the quantum algorithmic framework of Quantum Singular Value Transformations (QSVT). With QSVT one also has the ability to apply polynomials of linear operators onto an initial state. In contrast, however, to the here presented stochastic framework, QSVT is based on the idea of quantum signal processing (QSP) and general quantum embeddings. The basic insight of the QSP protocol is that one can implement almost arbitrary polynomials $p(H)$ of a hermitian operator H with a concatenation of a signal rotation operator $W(H)$ and a quantum signal processing rotation $e^{i\phi_k Z}$,

$$P(H) = \langle 0 | e^{i\phi_0} \prod_{k=1}^d W(H) e^{i\phi_k Z} | 0 \rangle. \quad (23)$$

In the context of this work the hermitian operator could be a Hamiltonian governing, for example, the real time evolution of a system of interest, while the polynomial

would be approximating the complex exponential function $P(z) \approx \exp(-itz)$. The approximate real time evolution would then proceed by applying the quantum signal processing sequence on an arbitrary initial state $|\psi_0\rangle$ and herald on the 0 measurement,

$$|\psi_t\rangle \approx \langle 0|e^{i\phi_0} \prod_{k=1}^d W(H)e^{i\phi_k Z}|0\rangle \otimes |\psi_0\rangle. \quad (24)$$

Instrumental to this technique is our ability to implement a unitary operator $W(H)$ such that $H = \langle 0|W(H)|0\rangle$, which is the topic of block encodings. One possibility to accomplish a block encoding for a Hamiltonian which can be described as a sum of Pauli operators is the technique of linear combination of unitaries (LCU). We need an ancillary qubit register of logarithmic size in the number of terms of the Hamiltonian and to prepare a state $|\Phi\rangle = \sum_{g \in S} \sqrt{p_g}|g\rangle$. We complement the ancillary qubit register with the computational qubit register of size n and apply the unitary Pauli operators of the Hamiltonian, controlled on the ancillary qubit register,

$$|\Phi\rangle \otimes |0\rangle \rightarrow \sum_{g \in S} \sqrt{p_g}|g\rangle \otimes g|0\rangle. \quad (25)$$

We finally apply the inverse of the unitary that prepared the state $|\Phi\rangle$ on the ancillary register. The entire procedure implements the correct signal rotation operator. However, the $|0\rangle$ state above as well as the signal processing rotation operator $e^{i\phi Z}$ are not a state respectively a rotation of a single qubit but rather their generalisations on the entire ancillary qubit register.

Comparing QSVT to the here presented stochastic framework, we can conclude that the “signal”, that means the information of the actual hermitian operator we want to apply, is encoded in the probabilities with which we apply the controlled rotations generated by Pauli operators rather than the state of an ancillary qubit

register. In turn the information about which polynomial of the hermitian operator we want to apply is encoded, first in the angles of the controlled rotations and second as the probabilities with which we apply the Z rotations on the single ancilla qubit that is needed for the stochastic framework, $\exp(i\frac{\pi}{4}z_a)$.

V. CONCLUSION

We have developed QCPP, a circuit-sampling approach for implementing a quantum channel that applies a polynomial of a Hamiltonian to an initial state. Each basic computational building block requires only controlled Pauli-rotation circuits for the Pauli terms appearing in the problem Hamiltonian. We have also identified the exponential sampling cost associated with the Jacobi-Anger expansion for target functions such as real-time and imaginary-time exponential functions. To overcome this obstruction, we constructed polynomials that realize a sample-query complexity trade-off: the sampling cost remains polynomially bounded while the additive approximation error achieves super-algebraic convergence with respect to the query complexity. These results provide a route toward quantum channel polynomial processing on NISQ and early fault tolerant quantum computers. Future work will demonstrate the experimental implementation of the algorithm on quantum hardware and extend the theoretical framework to interpolating a broader class of target functions using polynomially bounded circuit sampling cost.

ACKNOWLEDGEMENTS

We thank Stéphanie Cheylan, Oriël Kiss and Jinzhao Sun for useful and insightful discussions.

-
- [1] T. J. Yoder, G. H. Low, and I. L. Chuang, Fixed-point quantum search with an optimal number of queries, *Phys. Rev. Lett.* **113**, 210501 (2014).
 - [2] L. K. Grover, Fixed-point quantum search, *Phys. Rev. Lett.* **95**, 150501 (2005).
 - [3] P. W. Shor, Polynomial-time algorithms for prime factorization and discrete logarithms on a quantum computer, *SIAM Journal on Computing* **26**, 1484–1509 (1997).
 - [4] D. W. Berry, A. M. Childs, and R. Kothari, Hamiltonian simulation with nearly optimal dependence on all parameters, in *2015 IEEE 56th Annual Symposium on Foundations of Computer Science (IEEE, 2015)* p. 792–809.
 - [5] G. H. Low and I. L. Chuang, Hamiltonian Simulation by Qubitization, *Quantum* **3**, 163 (2019).
 - [6] A. W. Harrow, A. Hassidim, and S. Lloyd, Quantum algorithm for linear systems of equations, *Physical Review Letters* **103**, 10.1103/physrevlett.103.150502 (2009).
 - [7] J. M. Martyn, Z. M. Rossi, A. K. Tan, and I. L. Chuang, Grand unification of quantum algorithms, *PRX Quantum* **2**, 040203 (2021).
 - [8] L. N. Trefethen, *Approximation Theory and Approximation Practice, Extended Edition* (SIAM-Society for Industrial and Applied Mathematics, Philadelphia, PA, USA, 2019).
 - [9] L. R. Scott, *Numerical Analysis* (Princeton University Press, USA, 2011).
 - [10] Y. Dong, L. Lin, and Y. Tong, Ground-state preparation and energy estimation on early fault-tolerant quantum computers via quantum eigenvalue transformation of unitary matrices, *PRX Quantum* **3**, 040305 (2022).
 - [11] C.-F. Chen, M. J. Kastoryano, and A. Gilyén, An efficient and exact noncommutative quantum gibbs sampler (2023), arXiv:2311.09207 [quant-ph].

- [12] A. Gilyén, Y. Su, G. H. Low, and N. Wiebe, Quantum singular value transformation and beyond: exponential improvements for quantum matrix arithmetics, in *Proceedings of the 51st Annual ACM SIGACT Symposium on Theory of Computing*, STOC '19 (ACM, 2019) p. 193–204.
- [13] A. M. Childs and N. Wiebe, Hamiltonian simulation using linear combinations of unitary operations, *Quantum Information and Computation* **12**, 10.26421/qic12.11-12 (2012).
- [14] G. H. Low and N. Wiebe, Hamiltonian simulation in the interaction picture (2019), arXiv:1805.00675 [quant-ph].
- [15] D. Camps, L. Lin, R. V. Beeumen, and C. Yang, Explicit quantum circuits for block encodings of certain sparse matrices (2023), arXiv:2203.10236 [quant-ph].
- [16] G. H. Low, V. Kliuchnikov, and L. Schaeffer, Trading t gates for dirty qubits in state preparation and unitary synthesis, *Quantum* **8**, 1375 (2024).
- [17] Y. Kikuchi, C. Mc Keever, L. Coopmans, M. Lubasch, and M. Benedetti, Realization of quantum signal processing on a noisy quantum computer, *npj Quantum Information* **9**, 10.1038/s41534-023-00762-0 (2023).
- [18] M. Nibbi and C. B. Mendl, Block encoding of matrix product operators, *Physical Review A* **110**, 10.1103/physreva.110.042427 (2024).
- [19] F. D. Chiara, M. Nibbi, Y. Shen, and R. V. Beeumen, Efficient lcu block encodings through dicke states preparation (2025), arXiv:2507.20887 [quant-ph].
- [20] W. A. Simon, C. M. Gustin, K. Serafin, A. Ralli, G. R. Goldstein, and P. J. Love, Ladder operator block-encoding (2025), arXiv:2503.11641 [quant-ph].
- [21] D. Liu, W. Du, L. Lin, J. P. Vary, and C. Yang, An efficient quantum circuit for block encoding a pairing hamiltonian (2024), arXiv:2402.11205 [nucl-th].
- [22] R. Babbush, C. Gidney, D. W. Berry, N. Wiebe, J. McClean, A. Paler, A. Fowler, and H. Neven, Encoding electronic spectra in quantum circuits with linear t complexity, *Phys. Rev. X* **8**, 041015 (2018).
- [23] J. Lee, D. W. Berry, C. Gidney, W. J. Huggins, J. R. McClean, N. Wiebe, and R. Babbush, Even more efficient quantum computations of chemistry through tensor hypercontraction, *PRX Quantum* **2**, 030305 (2021).
- [24] D. S. Abrams and S. Lloyd, Simulation of many-body fermi systems on a universal quantum computer, *Phys. Rev. Lett.* **79**, 2586 (1997).
- [25] M. Suzuki, Decomposition formulas of exponential operators and Lie exponentials with some applications to quantum mechanics and statistical physics, *Journal of Mathematical Physics* **26**, 601 (1985).
- [26] A. M. Childs, Y. Su, M. C. Tran, N. Wiebe, and S. Zhu, Theory of trotter error with commutator scaling, *Physical Review X* **11**, 10.1103/physrevx.11.011020 (2021).
- [27] E. Campbell, Random compiler for fast hamiltonian simulation, *Phys. Rev. Lett.* **123**, 070503 (2019).
- [28] K. Nakaji, M. Bagherimehrab, and A. Aspuru-Guzik, qswift: High-order randomized compiler for hamiltonian simulation, arXiv preprint arXiv:2302.14811 (2023).
- [29] S. Lee and S. Choi, qshift: An adaptive sampling protocol for higher-order quantum simulation, arXiv preprint arXiv:2604.26263 (2026).
- [30] C.-F. Chen, H.-Y. Huang, R. Kueng, and J. A. Tropp, Concentration for random product formulas, *PRX Quantum* **2**, 040305 (2021).
- [31] P. Zeng, J. Sun, L. Jiang, and Q. Zhao, Simple and high-precision hamiltonian simulation by compensating trotter error with linear combination of unitary operations, *PRX Quantum* **6**, 10.1103/prxquantum.6.010359 (2025).
- [32] J. Sun and P. Zeng, Randomised composite linear-combination-of-unitaries: its role in quantum simulation and observable estimation (2025), arXiv:2506.15658 [quant-ph].
- [33] X. Wang, Y. Zhang, S. Hazra, T. Li, C. Shao, and S. Chakraborty, Randomized quantum singular value transformation (2025), arXiv:2510.06851 [quant-ph].
- [34] G. H. Low, T. J. Yoder, and I. L. Chuang, Methodology of resonant equiangular composite quantum gates, *Physical Review X* **6**, 10.1103/physrevx.6.041067 (2016).